

Source: Huawei, HiSilicon
Title: NR enhancements for DL MIMO
Agenda item: 4.1
Document for: Decision

1. Introduction

Massive MIMO is one of the key technologies to provide high spectrum efficiency in 5G systems. In Rel-18, the requirement on higher data rate and multi-user simultaneous transmission for eMBB scenarios is increasing, such as HD video streams, XR applications, high data rate UL transmissions and robust transmission in industry scenarios. To satisfy the high data rate requirement, massive MIMO for both FDD and TDD should be further enhanced in Rel-18, where Multi-TRP transmission is included.

In this contribution, we discuss massive MIMO enhancements in Rel-18, including the enhancements on FDD Massive MIMO, TDD Massive MIMO, where the Multiple TRPs scenarios is also included in the discussion. It's worth noting that the discussion on beam management part targeting on high frequency band is discussed in our companion contribution [1], and the enhancement of UL MIMO discussion is included in [2].

2. Motivations on Massive MIMO Enhancements

2.1. TDD Massive MIMO Enhancements

Massive MIMO has been already widely deployed in TDD scenarios in 5G, while Massive MIMO is one of the key technologies to provide high spectrum efficiency for 5G. For the existing Massive MIMO deployment and potential deployment, to further enhance Massive MIMO in Rel-18 is beneficial to provide higher spectrum efficiency for the coming higher data rate scenarios while the penetration of 5G users is quickly increasing and new applications for high data rate requirements are on the road, such as HD video and AR/VR. There are at least following aspects need to be further investigated in Massive MIMO for higher spectrum efficiency in Rel-18.

At first, it is known that the granularity of precoding is restricted as wideband, 4 or 2 RBs in Rel-15 ~ Rel-17. However, in the some practical deployments, the channels are generally with large frequency selective. The angle power profile of these channels show the beam varies within PRG (4 or 2RBs). So, current precoding granularity cannot adapt the channel and limit the precoding accuracy for MIMO transmission.

And then, the multi-users pairing capability is restricted to no more than 12 layers in Rel-15~17 as only 12 orthogonal DMRS ports are defined. But for the use case of dense UEs, video cases, XR and multi-TRP cases, the MU pairing layers will exceed 12. In addition, in the UL scenarios as discussed in [2], such as industry applications, there are much more devices are for UL simultaneous transmission with high data rate. In these cases, current 12 orthogonal DMRS are not sufficient to support the high order MU MIMO.

Furthermore, for supporting the increasing UL traffics in video or XR applications, and low latency requirement for UL transmission, the SRS capacity need to be enhanced but without loss of PUSCH capacity/resources. Furthermore, inter-cell interference for SRS is an important issue need to be addressed, especially for the case of Multi-TRP, which is not well investigated in previous releases in NR. Therefore, in our understanding, the enhancements of TDD Massive MIMO in Rel-18 are expected to provide much more accurate precoding, capability on interference mitigation, better supporting on mobility and better multi-user pairing capability.

2.2. FDD Massive MIMO Enhancements

NR supports abundant sub-3GHz spectrum for FDD, which includes 14 NR operating bands and spreads over 700MHz, 800MHz, 900MHz, 1.8GHz, 2.1GHz and 2.6GHz. Typically, almost all the operators in the world own multiple sub-3GHz bands for cellular deployment. Especially for 1.8GHz and 2.1GHz, hundreds of operators have deployed FDD network in these two bands. Re-farming these sub-3GHz bands to NR would improve the coverage of NR, the spectrum efficiency of sub-3GHz, the NR RTT latency, and the network energy efficiency.

To support re-farming of FDD bands to 5G, massive MIMO is one of the key technologies, which can provide high data rate to satisfy the requirement for 5G users' experience. It is known that, in Rel-17, CSI feedback with FDD partial reciprocity based codebook can significantly improve spectral efficiency and network capacity compared to FDD MIMO

in previous releases, where Rel-17 NR FDD 32Tx exceeds more than 4 times the performance of Rel-15 NR FDD 4Tx with type-I codebook.

However, in some scenarios or new applications, the massive MIMO are not well designed, such as high mobility cases, multiple-TRP with coherent joint transmission cases, etc. For mobility cases, due to large Doppler shift, the CSI from feedback will be aged. How to address the impact of Doppler shift for CSI feedback in mobility cases is one of aspects could be discussed in Rel-18. For multi-TRP cases, it is known that C-RAN structure is widely used in practical scenarios due to low cost and fast deployment, where coherent joint transmission can be enabled in such cases. The FDD CSI design was only for non-coherent joint transmission in previous releases. In addition, the precoding granularity enhancement and Rel-17 leftover also can be further investigated. How to improve the system performance for coherent joint transmission also could be discussed in Rel-18.

3. Potential enhancements for DL MIMO in Rel-18

3.1. Enhancements for MIMO precoding for TDD and FDD

Precoding is the core technology for massive MIMO system. Accurate precoder should be designed to fit into the channel characteristic. Therefore, it can effectively reduce the inter-layer/inter-user interference, and maximize the SINR of the receiver. For the MIMO-OFDM system, frequency selective fading is an important factor restricting the performance, especially for the channel with high delay spread. As show in Figure 1 (a), for low delay spread 100ns, the channel of single TRP is relatively flat in frequency. The strongest beams corresponding to different 1/2 PRB (6 REs) are the same. When the delay spread increases to 300ns, the strongest beams are different even within 1 PRB (Figure 1(b)). For multi-TRP scenario e.g., coherent joint transmission (CJT) system, the frequency selective fading is more severe than single TRP scenario because the effective joint channel matrix is constructed by channels of multiple TRPs, as shown in Figure 1(c). The strongest beam varies more significantly with the constructed channel although the delay spread is small with 100ns per TRP

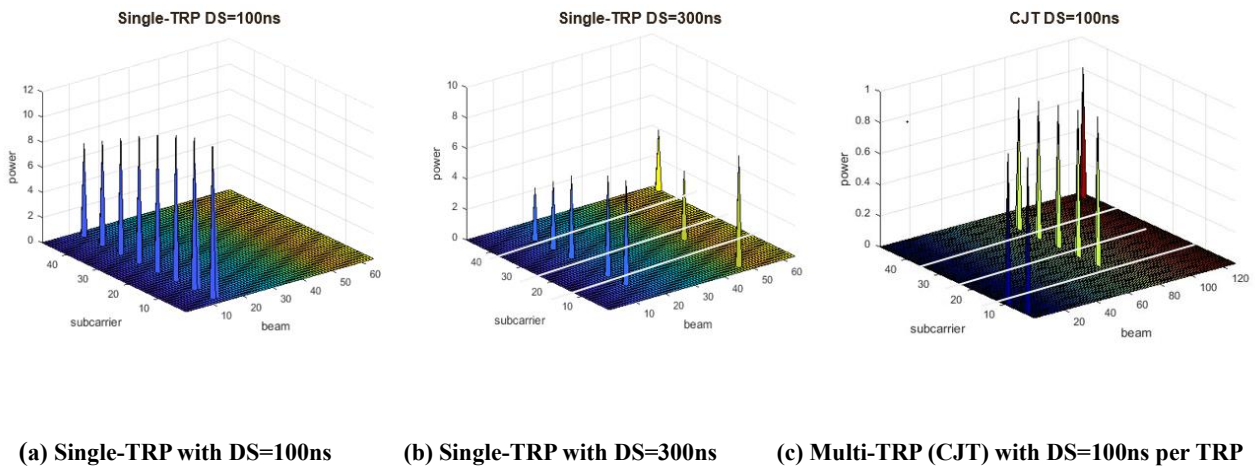


Figure 1. The distribution of the strongest beam in different frequency-domain subbands (CDL-B channel)

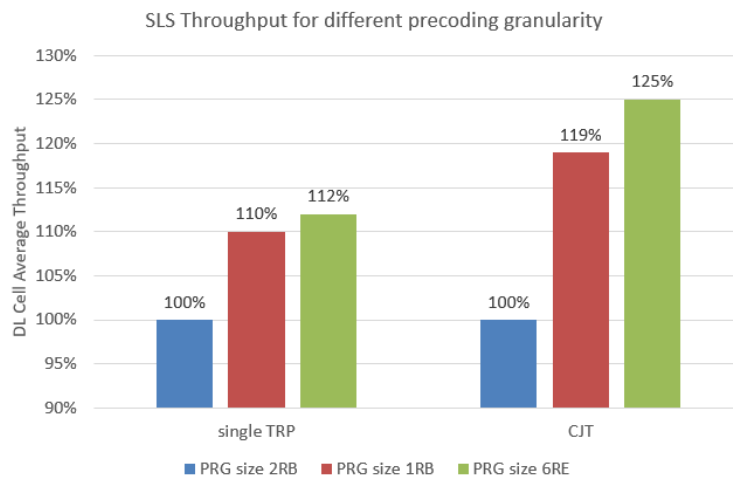


Figure 2. Performance evaluation for different precoding granularity

In current NR system, the precoding granularity (PRG size) is wideband, or 4 PRBs or 2 PRBs. This precoding granularity is too coarse to adapt to the high frequency selective channel e.g., delay spread with 300ns. As shown in Figure 2, finer granularity precoding provides obvious performance gain as it can overcome the frequency selective fading, where more than 10% gain can be observed from single TRP case, and about 20% gain can be obtained in multi-TRP cases. The simulation parameters can be found in the Appendix A. It's worth noting that real channel estimation is assumed in the evaluation.

To further improve the MIMO performance, high resolution precoding for high frequency selective fading could be discussed in Rel-18. And we have the following proposal

Proposal 1: To further improve DL MIMO performance in highly frequency selective channels including multi-TRP scenario, finer precoding granularity could be included in Rel-18.

3.2. DMRS enhancement for TDD and FDD

With the explosive growth of 5G equipment and the development of high data rate services (e.g. XR applications), improvement of the number of transmission streams is the key direction of MIMO evolution, which provide more data rate with the same resources. In UL transmissions, there is requirement on multi-users simultaneous transmission with high data rate, especially in industrial scenarios, which is discussed our companion contribution [2]. Moreover, in multi-TRP scenarios, more users are possibly scheduled by MU transmission, especially in the case of coherent joint transmission (CJT).

In the preliminary simulation, the distribution of transmission layers N_{layer} from SLS is shown in Figure.3 for multi-TRP with coherent joint transmission. In the evaluation, 64Tx is assumed in gNB side and the RU is assumed as 70% for burst buffer case. Other detailed simulation assumptions can be found in Appendix-B for single TRP (Table 6-3) and multi-TRP cases (Table 6-4). It can be seen that the number of MU layers N_{layer} is greater than 12 for burst buffer traffic with coherent joint transmission. In Rel-15~17, it can only support up to 12 orthogonal DMRS ports. So, to support more than 12 DMRS ports could be discussed in Rel-18.

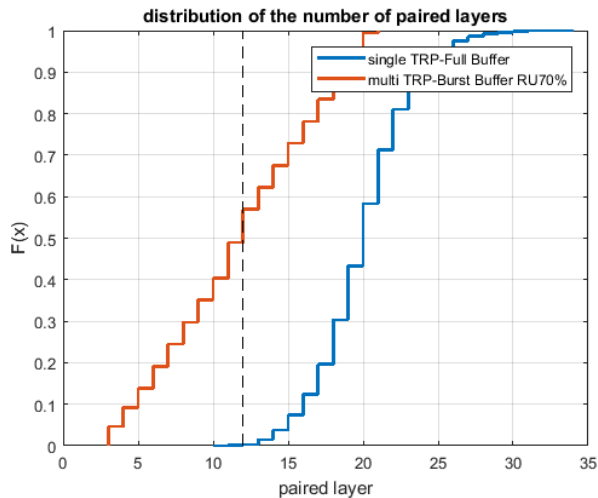


Figure 3. Distribution of transmission layers for MU-MIMO for coherent joint transmission

At present, NR supports two types of DMRS resource mapping. For Type 1 DMRS, it can support up to 8 orthogonal ports; for Type 2 DMRS, up to 12 orthogonal ports are supported. One possible way to expand the number of orthogonal DMRS ports is to increase the time-frequency resources occupied by DMRS. This method will obviously increase the overhead of DMRS and reduce the spectral efficiency of the system.

Another possible method is to use scrambling IDs to generate non-orthogonal DMRS ports, such as up to 24 non-orthogonal DMRS ports can be used with modifying the quantity $n_{SCID} \in \{0, 1\}$ in the sequence generation. However, this method will bring high interference, especially in the scenario of high user correlation, due to the doubled sequences are not optimized for low correlation.

Figure 4(a) shows the BLER performance of ideal channel estimation and non-orthogonal DMRS ports with real channel estimation for 16 layers and MCS 17. The simulation parameters can be found in the Appendix C. It can be observed that the non-orthogonal DMRS ports (12 ports correspond to $n_{SCID} = 0$, the other 4 ports correspond to $n_{SCID} = 1$) will lead to an obvious error floor. The performance loss is about 3.5dB compared to ideal channel estimation. The loss will grow larger and larger with the increase of the number of data streams as shown in Figure 4. For 24 layers and MCS 14, the

performance gap between channel estimation with non-orthogonal DMRS ports (12 ports correspond to $n_{\text{SCID}} = 0$, the other 12 ports correspond to $n_{\text{SCID}} = 1$) and ideal channel estimation is larger than 4dB.

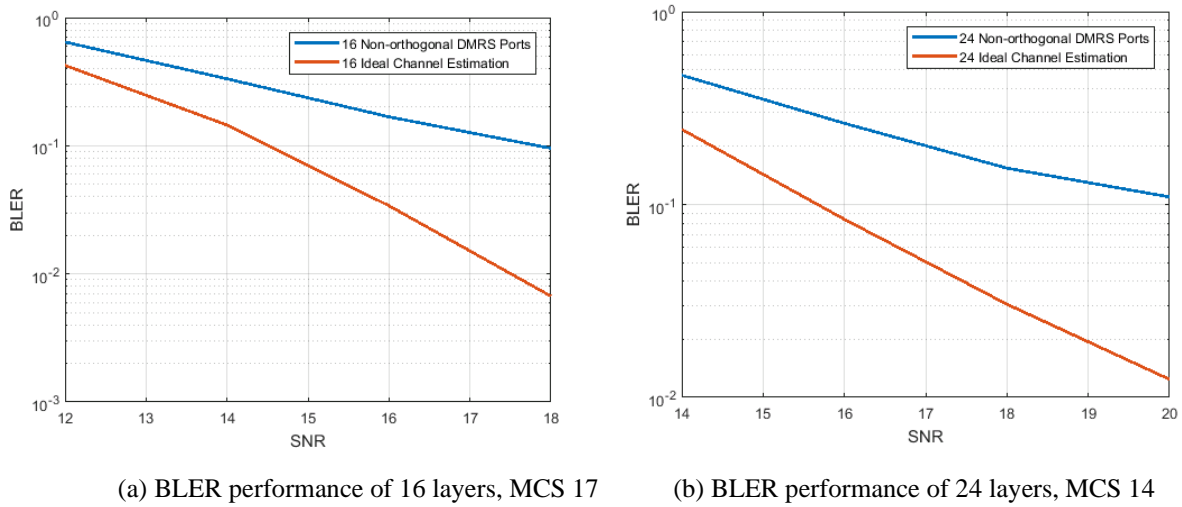


Figure 4. The performance of non-orthogonal DMRS ports generated by different value of n_{SCID}

To support more than 12 layers in Rel-18, two potential ways are worth investigating in Rel-18. One is introduce orthogonal cover codes to provide more orthogonal DMRS ports, another way is to introduce lower correlation DMRS sequences to reduce interference. But, the enhancements of DMRS in Rel-18 are expected without additional time-frequency resources, and also compatible with the existing DMRS ports.

Proposal 2: To satisfy the requirement of high traffic, DMRS enhancement supporting more than 12 ports could be included in Rel-18:

- without additional time-frequency resources
- compatible with the existing DMRS ports

3.3. SRS enhancements for TDD

TDD system highly rely on SRS to acquire the channel information, but the performance of SRS suffers from two main factors. One factor is SRS capacity which determines the periodicity of SRS. The performance degrades by $\sim 30\%$ if SRS periodicity increases from 20ms to 160ms as shown in Figure 5, where the velocity is assumed with 3km/h. The detailed evaluation assumptions are listed in Appendix-C. With increasing capacity requirements for new uplink traffic e.g., XR, more uplink resources should be reserved for uplink traffic and cannot be allocated for SRS capacity enhancement. Therefore, SRS capacity enhancement should be achieved with limited uplink resources.

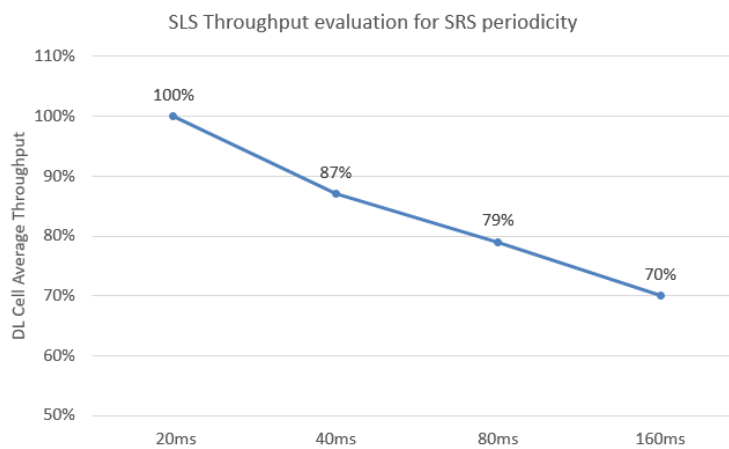


Figure 5. Throughput evaluations for different SRS periodicity

R17 has introduced partial SRS for SRS capacity enhancement in which SRS is only transmitted some but not all PRBs of the hopping band. The main idea of R17 partial SRS is to sound partial continuous PRBs within the full band, and the unsounded PRBs can be obtained by utilizing frequency-domain channel interpolation. Our R17 contributions have

demonstrated the DL performance improvement of R17 partial SRS with 2 and 4 times (corresponding to partial factor PF=2 and 4, respectively) capacity enhancement. However, the channel correlation between the sounded PRBs and the unsounded PRBs is related to their frequency distance. The performance gain of partial SRS is limited if large partial factors or wider system bandwidth is considered, such as PF=8 or 100M system bandwidth.

To further enhance SRS capacity in the case of dense users, new SRS design needs to be considered through reducing SRS overhead based on the sparse characteristic of multi-path channel or producing additional orthogonal SRSs with zero auto/cross correlation zones, which can guarantee the channel estimation accuracy. As an example, one can increase the number of orthogonal SRSs 4 to 8 times by modifying NR SRS resource allocation, so that fewer (4 to 8 times) number of subcarriers per SRS are used, while the corresponding mapping patterns are selected according to the principle of compressive sensing in order to maintain the same quality of the corresponding channel estimates as obtained by the existing NR SRSs.

In the preliminary evaluation, R18 with PF=8 can achieve more than 10% gain compared to R17 partial SRS with PF=4 as shown in Figure 6, where the same multiplexing capacity is assumed. The simulation assumption can be found in Appendix D in Table 6-6.

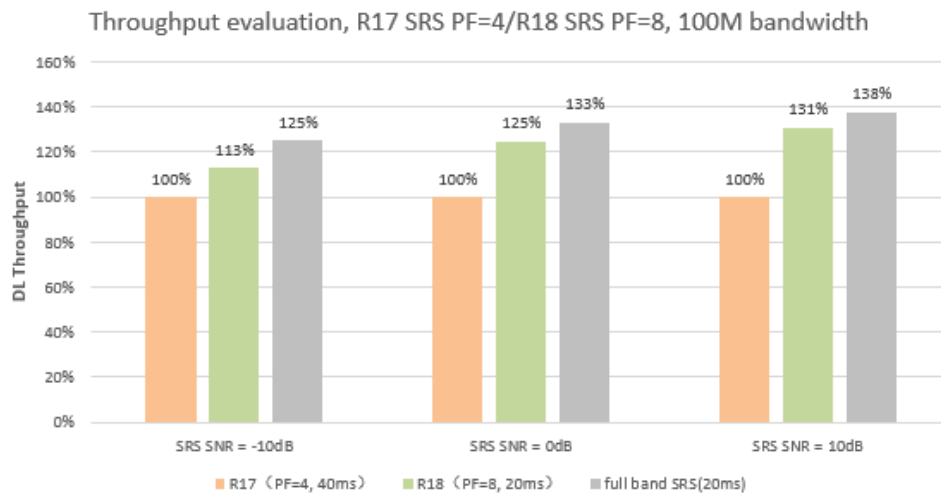


Figure 6. Throughput evaluation for R18 SRS Capacity Enhancement

Proposal 3: Enhancing the SRS capacity without reducing channel estimation performance could be included in Rel-18 scope.

The second factor is regarding to inter-cell interference for SRS. The current interference suppression method is to whiten the coloured interference by low correlation sequences. Considering more UEs with more antennas served in NR, interference on SRS increases as their collision probability increases. The sequence correlation is limited by sequence length and this is hard to further improve, so interference has become an issue limiting SRS performance. The impact of interference in single TRP scenario is shown in Figure 7, and it can be seen there is 37% performance gap between SRS with inter-cell interference and SRS with ideal inter-cell interference mitigation, where the evaluation assumptions are provided in Appendix-D in Table 6-7.

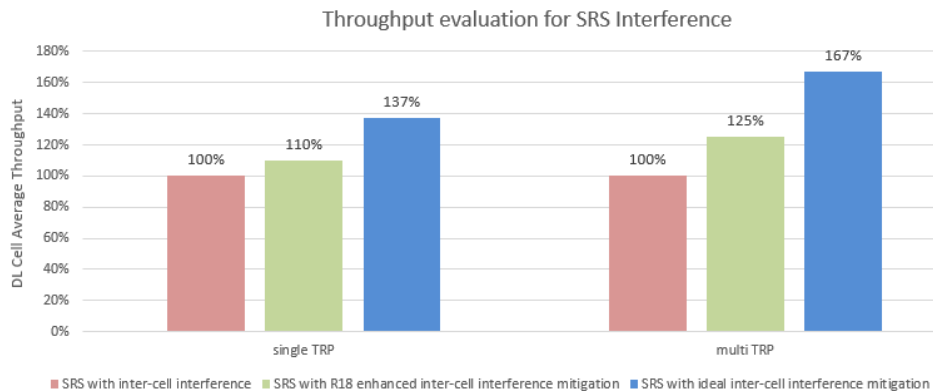


Figure 7. Throughput evaluations for SRS interference

The interference problem is even worse in multi-TRP scenario, since SRS signals should be received and estimated by multiple TRPs to enable downlink Coherent Joint Transmission (CJT) transmission. The distributed TRPs will cause uneven RSRP of received SRS signals as shown in Figure 8. In Figure 7, there is 67% performance gap from current SRS with inter-cell interference and the ideal case with mitigated all inter-cell interference for SRS. The performance decrease is mainly caused by poor estimation of SRS signal in multi-TRP case.

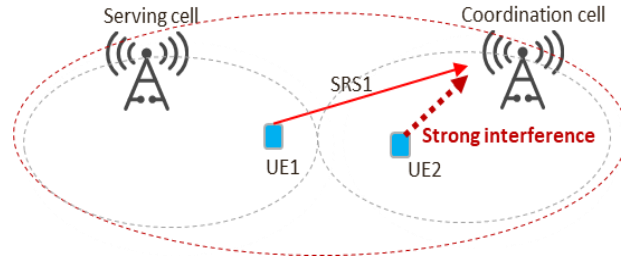


Figure 8. Strong inter-cell interference in multi-TRP scenarios for SRS

One simple method to reduce the inter-cell interference is assigning orthogonal SRS resources among neighbouring cells, but this method will reduce the available SRS resources per cell and increases SRS periodicity which leads to channel aging problem as shown in Figure 9. For certain SRS periodicity, if the channel aging problem is dominant, using this method cannot improve the performance at all.

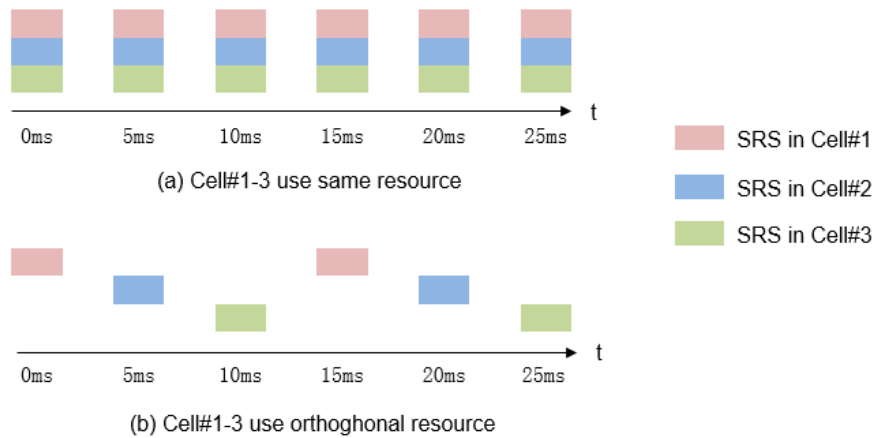


Figure 9. Longer SRS periodicity with orthogonal resource among cooperation set

Two aspects can be considered to mitigate the inter-cell interference for SRS. One aspect is to weaken the SRS interference strength, the other aspect is to decrease the correlation between interfering SRS and desired SRS. For the first aspect, SRS can be scheduled with directional transmission, i.e., beamformed SRS. For the second aspect, more SRS interference whitening method should be consider, such as SRS sequences with lower correlation. The third aspect is to introduce SRS interference randomization. In Figure-7, R18 SRS enhancement is based on interference whitening with lower sequence correlation, which shows 10%~25% gain for single TRP and multi-TRP, respectively.

Proposal 4: Reducing inter-cell interference for SRS could be included in the scope of Rel-18.

3.4. CSI Enhancement for Mobility Cases for FDD

During the conventional procedure of CSI acquisition, gNB use the latest CSI reported by UEs for DL precoder until next precoder is enabled i.e., precoding is constant during t_2 with a delay of t_1 .

- ✓ t_1 : delay of CSI acquisition (including scheduling delay potentially)
- ✓ t_2 : time period of CSI update

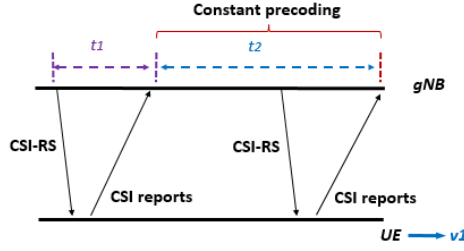


Figure 10. CSI delay during CSI acquisition procedure

It is well known that CSI ageing would introduce performance loss, especially in the case of mobility due to high Doppler. To guarantee the performance in the mobility case, one potential solution is CSI prediction.

Conventionally, legacy PMI feedback targets for approaching ideal eigenvector(s) for each subband at a reporting instant. The time domain correlation information between different instants with legacy PMI feedback is difficult to obtain, because different channel realizations of H at different time instants ($H_1 \sim H_T$) would lead to different left eigenvector U ($U_1 \sim U_T$). Then the time domain correlation information between $H_1 \sim H_T$ may not be kept in $V_1 \sim V_T$, i.e., the Doppler shift and spread of real channel would be disrupted by unitary matrix U for each time instants.

$$H = UAV^H$$

$$V = H^H UA^{-1}$$

$$[v_1, v_2, \dots, v_n] = H^H [u_1, u_2, \dots, u_n] \begin{bmatrix} a_1 & \dots & 0 \\ \vdots & \ddots & \vdots \\ 0 & \dots & a_n \end{bmatrix}^{-1}$$

$$v_1 = H^H u_1 \frac{1}{a_1}$$

To obtain accurate time-domain channel correlation information at gNB side while considering CSI feedback overhead, joint CSI feedback for multi-instant could be considered.

In addition, CSI compression via Doppler information can also be used in the low mobility case to reduce the CSI feedback overhead.

Proposal 5: CSI enhancement for mobility scenario considering CSI compression via time domain correlation could be in the scope for Rel-18.

3.5. FDD MIMO enhancement for Multiple TRP



Figure 11. Multi-TRP coordinated joint transmission

With the acceleration of C-RAN network deployment, large scale multi-TRP coherent joint transmission (CJT) can be supported in practical system with higher probability than before. With centralized interference suppression in larger coordination set, a large improvement in the network throughput can be obtained, compared with non-coherent joint transmission (NCJT).

In FDD system, codebook enhancement only targets for non-coordinated or non-coherent joint transmissions up to Rel-17. For the multi-TRP or multi-panel case, only type I multi-panel codebook is specified in R15, which cannot satisfy the requirement of CJT. High resolution codebook for CJT could be investigated in Rel-18.

Furthermore, with large number of antennas in cooperated TRPs and high interference suppression by CJT, there are more MU MIMO transmission layers, but only twelve orthogonal DMRS layers are supported in current specifications. So, more than 12 layers of DMRS design need to be investigated in FDD coherent joint transmission cases in Rel-18.

CSI enhancement for Coherent joint transmission (CJT)

CSI measurement and feedback was designed for single cell or non-coherent joint transmission but not for coherent joint transmission before. For the multi-TRP or multi-panel case, only type I multi-panel codebook is specified in R15, which cannot satisfy the requirement of CJT. High resolution CSI design for CJT is required in Rel-18.

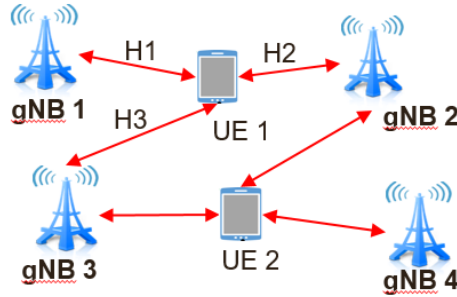


Figure 12. CSI feedback for coherent joint transmission

In CJT scenarios, the information of correlation between different channels from different TRPs (H1, H2, H3 in Fig. 12 as an example) need to be included in CSI measurement/reporting design, where both large scale and small scale channel properties should be considered. Large scale channel property should be considered due to joint precoding at gNB size. For the small channel property, simple single phase, as in in multi-panel codebook specified in R15, is not enough to represent the channel correlations between transmit antennas of two TRPs. In practical scenarios with multiple transmission rays, high resolution codebook for multi-TRP/panel is required, e.g., assuming N transmit antennas for each TRP, then N^2 phase are needed.

To enable gNB acquire high resolution channel correlations between transmit antennas of multiple TRPs, CSI feedback based on the joint channel of multi-TRP ($[H_1^T, H_2^T, H_3^T]^T$ for the case of 3 TRPs) can be considered. The channels of the UE to different TRPs may be unrelated due to non-overlapping transmission rays, and separate CSI compression for each TRP while joint coefficient reporting can be considered, which can also support flexible multi-TRP CSI feedback with different number of TRPs for CJT.

Furthermore, the interference hypotheses are also different in CJT cases compared to single TRP and NCJT transmission. The interference from UEs within cooperated TRPs can be suppressed by precoding, while only the interference from the TRPs out of cooperation requires specific interference measurement.

In the preliminary evaluation, as shown in Fig 13, coherent joint transmission with joint channel information (i.e., $[H_1^T, H_2^T, H_3^T]^T$ for the case of 3 TRPs) obtain more than 40%~50% gain compared to Rel-17 non-coherent joint transmission. The main simulation setting is listed in Appendix D.

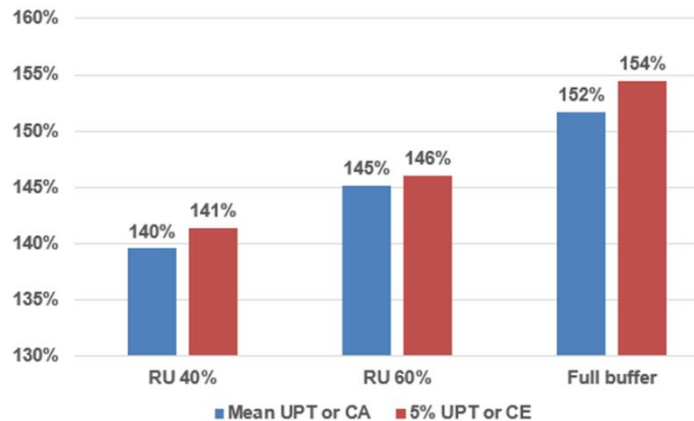


Figure 13. Performance gain of coherent joint transmission with high resolution multi-TRP codebook compared to R17 Non-coherent joint Transmission

Proposal 6: Enhancements on CSI measurement and feedback for FDD Coherent Joint Transmission (CJT) could be in the scope of Rel-18 MIMO enhancements.

3.6. Rel-17 leftover discussion

In Rel-17, FDD channel reciprocity is well investigated in the CSI feedback, which provided obvious performance gain compared to conventional CSI design.

With the enhancements on precoding mentioned in Section 3.1.1, the requirement on the resolution of CSI increases. So, it could be beneficial to enhance FDD CSI based on Rel-17, which could be studied in Rel-18. In addition, there is some discussion on CSI-RS overhead reduction in Rel-17. In Rel-17 FDD CSI use, aperiodic CSI-RS is a good tradeoff between CSI-RS overhead and performance. By using periodic CSI-RS for such cases, the overhead reduction could be further studied in Rel-18.

4. Conclusions

In this paper we provided justifications for supporting NR massive MIMO enhancement in Rel-18. In our understanding, the following directions should be included in the scope of enhancements of massive MIMO in Rel-18 to satisfy the requirements of high data rate. We have the following proposals

Proposal 1: To further improve DL MIMO performance in highly frequency selective channels including multi-TRP scenario, finer precoding granularity could be included in Rel-18.

Proposal 2: To satisfy the requirement of high traffic, DMRS enhancement supporting more than 12 ports could be included in Rel-18:

- without additional time-frequency resources
- compatible with the existing DMRS ports

Proposal 3: Enhancing the SRS capacity without reducing channel estimation performance could be included in Rel-18 scope.

Proposal 4: Reducing inter-cell interference for SRS could be included in the scope of Rel-18.

Proposal 5: CSI enhancement for mobility scenario considering CSI compression via time domain correlation could be in the scope for Rel-18.

Proposal 6: Enhancements on CSI measurement and feedback for FDD Coherent Joint Transmission (CJT) could be in the scope of Rel-18 MIMO enhancements.

5. References

- [1] RWS-210438, “NR FR2 enhancements”, Huawei, HiSilicon
- [2] RWS-210436, “NR uplink boosting”, Huawei, HiSilicon

6. Appendix

Appendix A: System simulation parameters for MIMO precoding enhancement

Table 6-1 Simulation assumptions of SLS for single-TRP

Parameter	Value
Duplex, Waveform	TDD, OFDM
Carrier Frequency	3.5G
Channel Model	According to the TR 38.901
Scenario	UMa with 200 m ISD
Antenna setup and port layouts at gNB	(M, N, P, Mg, Ng; Mp, Np) = (8,8,2,1,1,4,8), (dH, dV) = (0.5, 0.8)
Antenna setup and port layouts at UE	(M, N, P, Mg, Ng; Mp, Np) = (1,2,2,1,1,1,2), (dH, dV) = (0.5, 0.5)
BS Tx power	46 dBm
BS antenna height	25 m
UE receiver noise figure	9dB

Numerology	14 OFDM symbol slot, 30kHz SCS
Modulation	up to 256QAM
Bandwidth	20 MHz
MIMO scheme	SU/MU-MIMO with rank adaptation Maximum rank = 4 per UE
Traffic model	FTP model 3 with packet size 0.5 Mbytes.
RU	70%
UE distribution	80% indoor (3km/h), 20% outdoor (30km/h)
UE receiver	MMSE-IRC
Network Layout	7*3 cell, 30 UEs pre cell
Precoding granularity	4RB / 1RB / 0.5RB
Precoding method	EZF
Error modeling for SRS channel estimation	Table A.1-2 of TR 36.897 $\Delta = 9$ dB is assumed
Error modeling for DL DMRS channel estimation	Based on SINR loss evaluated from LLS

Table 6-2 Simulation assumptions of SLS for multi-TRP

Parameter	Value
Duplex, Waveform	TDD, OFDM
Carrier Frequency	3.5G
Channel Model	According to the TR 38.901
Scenario	UMa with 200 m ISD
Antenna setup and port layouts at gNB	(M, N, P, Mg, Ng; Mp, Np) = (8,8,2,1,1,4,8), (dH, dV) = (0.5, 0.8)
Antenna setup and port layouts at UE	(M, N, P, Mg, Ng; Mp, Np) = (1,2,2,1,1,1,2), (dH, dV) = (0.5, 0.5)
BS Tx power	46 dBm
BS antenna height	25 m
UE receiver noise figure	9dB
Numerology	14 OFDM symbol slot, 30kHz SCS
Modulation	up to 256QAM
Bandwidth	5 MHz
MIMO scheme	SU/MU-MIMO with rank adaptation Maximum rank = 4 per UE
Traffic model	FTP model 3 with packet size 0.5 Mbytes.
RU	70%
UE distribution	80% indoor (3km/h), 20% outdoor (30km/h)
UE receiver	MMSE-IRC
Network Layout	7*3 cell, 10 UE pre cell
Precoding granularity	4RB / 1RB / 0.5RB
Precoding method	CJT based on WMMSE
Error modeling for SRS channel estimation	Table A.1-2 of TR 36.897 $\Delta = 9$ dB is assumed
Error modeling for DL DMRS channel estimation	Based on SINR loss evaluated from LLS

Appendix B: System level simulation parameters for DMRS enhancement

Table 6-3 Simulation assumptions of SLS for single-TRP with full buffer traffic model

Parameter	Value
Duplex, Waveform	TDD, OFDM
Carrier Frequency	3.5G
Channel Model	According to the TR 38.901
Scenario	Uma with 200 m ISD
Antenna setup and port layouts at gNB	(M, N, P, Mg, Ng; Mp, Np) = (8,8,2,1,1,4,8). (dH, dV) = (0.5, 0.8)
Antenna setup and port layouts at UE	(M, N, P, Mg, Ng; Mp, Np) = (1,2,2,1,1,1,2), (dH, dV) = (0.5, 0.5)
BS Tx power	46 dBm
BS antenna height	25 m
UE receiver noise figure	9dB
Numerology	14 OFDM symbol slot, 30kHz SCS
Modulation	up to 256QAM
Bandwidth	20 MHz
MIMO scheme	SU/MU-MIMO with rank adaptation Maximum rank = 4 per UE
Traffic model	Full buffer
UE distribution	80% indoor (3km/h), 20% outdoor (30km/h)
UE receiver	MMSE-IRC
Network Layout	7*3 cell, 10 UE per cell
Precoding granularity	4RB / 1RB / 0.5RB
Precoding method	EZF
SRS channel estimation	Ideal channel estimation
DL DMRS channel estimation	Ideal channel estimation

Table 6-4 Simulation assumptions of SLS for multi-TRP with non-full buffer traffic model

Parameter	Value
Duplex, Waveform	TDD, OFDM
Carrier Frequency	3.5G
Channel Model	According to the TR 38.901
Scenario	Uma with 200 m ISD
Antenna setup and port layouts at gNB	(M, N, P, Mg, Ng; Mp, Np) = (8,8,2,1,1,4,8). (dH, dV) = (0.5, 0.8)
Antenna setup and port layouts at UE	(M, N, P, Mg, Ng; Mp, Np) = (1,2,2,1,1,1,2), (dH, dV) = (0.5, 0.5)
BS Tx power	46 dBm
BS antenna height	25 m
UE receiver noise figure	9dB
Numerology	14 OFDM symbol slot, 30kHz SCS
Modulation	up to 256QAM
Bandwidth	5 MHz
MIMO scheme	SU/MU-MIMO with rank adaptation Maximum rank = 4 per UE
Traffic model	FTP model 3 with packet size 0.5 Mbytes.
Traffic load (Resource utilization)	70%
UE distribution	80% indoor (3km/h), 20% outdoor (30km/h)
UE receiver	MMSE-IRC
Network Layout	7*3 cell, 10 UE pre cell
Precoding granularity	4RB

Precoding method	CJT based on WMMSE
SRS channel estimation	Ideal channel estimation
DL DMRS channel estimation	Ideal channel estimation

Appendix C: Link level simulation parameters for DMRS enhancement

Table 6-5 Simulation assumptions of LLS for DMRS enhancement

Parameter	Value
Carrier Frequency	3.5G
Channel Model	CDL-B in TR 38.901
Delay Spread	129ns / 363ns
BS antenna configuration	(M, N, P, Mg, Ng; Mp, Np) = (8,8,2,1,1;4,8), (dH, dV) = (0.5, 0.8)
UE antenna configuration	(M, N, P, Mg, Ng; Mp, Np) = (1,2,2,1,1;1,2), (dH, dV) = (0.5, 0.5)
MIMO scheme	MU-MIMO
Modulation	64QAM
MCS	MCS 12 / 17
Bandwidth	20 MHz
Numerology	14 OFDM symbol slot, 30kHz SCS
MIMO Rank	Maximum rank = 2 (Rank fixed)
UE speed	3km/h
Precoding granularity	4RB
Precoding method	EZF
DMRS	Type 2 DMRS, two-symbols
DL DMRS channel estimation	MMSE channel estimation

Appendix D: System simulation parameters for SRS enhancement

Table 6-6 Simulation assumptions of SLS for SRS enhancement for single TRP

Parameter	Value
Duplex, Waveform	TDD, OFDM
Carrier Frequency	3.5G
Channel Model	According to the TR 38.901
Scenario	Uma with 200 m ISD
BS antenna configuration	(M, N, P, Mg, Ng; Mp, Np) = (8,8,2,1,1,4,8), (dH, dV) = (0.5, 0.8)
UE antenna configuration	(M, N, P, Mg, Ng; Mp, Np) = (1,2,2,1,1,1,2), (dH, dV) = (0.5, 0.5)
BS Tx power	46 dBm
BS antenna height	25 m
UE receiver noise figure	9dB
Numerology	14 OFDM symbol slot, 30kHz SCS
Modulation	up to 256QAM
Bandwidth	100 MHz
MIMO scheme	SU/MU-MIMO with rank adaptation Maximum rank = 4 per UE
Traffic model	FTP model 3 with packet size 0.5 Mbytes.
UE distribution	80% indoor (3km/h), 20% outdoor (30km/h)
UE receiver	MMSE-IRC
Network Layout	7*3 cell, 30 UEs per cell

Precoding granularity	4RB
Precoding method	EZF
SRS period	20ms / 40ms / 80ms / 160ms
SRS antenna switching	2T4R
SRS measure delay	1 ms

Table 6-7 Simulation assumptions of SLS for SRS enhancement

Parameter	Value
Duplex, Waveform	TDD, OFDM
Carrier Frequency	3.5G
Channel Model	According to the TR 38.901
Scenario	Uma with 200 m ISD
BS antenna configuration	(M, N, P, Mg, Ng; Mp, Np) = (8,8,2,1,1,4,8), (dH, dV) = (0.5, 0.8)
UE antenna configuration	(M, N, P, Mg, Ng; Mp, Np) = (1,2,2,1,1,1,2), (dH, dV) = (0.5, 0.5)
BS Tx power	46 dBm
BS antenna height	25 m
UE receiver noise figure	9dB
Numerology	14 OFDM symbol slot, 30kHz SCS
Bandwidth	16 RB
MIMO scheme	MU-MIMO with fixed Rank 1 per UE
Traffic model	FTP model 3 with packet size 0.5 Mbytes.
RU	70%
UE distribution	80% indoor (3km/h), 20% outdoor (30km/h)
UE receiver	MMSE-IRC
Network Layout	7*3 cell, 4 UE per cell
Precoding granularity	2RB
Precoding method	EZF for single TRP, WMMSE for CJT
SRS period	5ms
SRS configuration	2 Combs, 4 CS

Appendix E: System simulation parameters for FDD CJT enhancement

Table 6-8 Simulation assumptions of SLS for FDD CJT enhancement

Parameter	Value
Duplex, Waveform	FDD, OFDM
Carrier Frequency	2.1G
Channel Model	According to the TR 38.901
Scenario	Uma with 300 m ISD
Antenna setup and port layouts at gNB	(M, N, P, Mg, Ng; Mp, Np) = (8,8,2,1,1,2,8), (dH, dV) = (0.5, 0.8)
Antenna setup and port layouts at UE	(M, N, P, Mg, Ng; Mp, Np) = (1,2,2,1,1,1,2), (dH, dV) = (0.5, 0.5)
BS Tx power	46 dBm
BS antenna height	25 m
UE receiver noise figure	9dB
Numerology	14 OFDM symbol slot, 30kHz SCS
Modulation	up to 256QAM
Bandwidth	10 MHz

MIMO scheme	SU/MU-MIMO with rank adaptation Maximum rank = 4 per UE
Traffic model	FTP model 1 with packet size 0.5 Mbytes.
UE distribution	80% indoor (3km/h), 20% outdoor (30km/h)
UE receiver	MMSE-IRC
Network Layout	7*3 cell, 30 UEs pre cell
Precoding granularity	2RB